PHYSICAL REVIEW B
CONDENSED MATTER

THIRD SERIES, VOLUME 48, NUMBER 9 1 SEPTEMBER 1993-I

# Freezing and melting of fluids in porous glasses

Eric Molz
*Department of Physics, University of Alberta, Edmonton, Alberta, Canada T6G 2J1*

Apollo P. Y. Wong* and M. H. W. Chan
*Department of Physics, Pennsylvania State University, 104 Davey Laboratory, University Park, Pennsylvania 16802*

J. R. Beamish
*Department of Physics, University of Alberta, Edmonton, Alberta, Canada T6G 2J1*
(Received 5 February 1993)

We have studied the freezing and melting of a number of cryogenic fluids (hydrogen, neon, oxygen, and argon) confined in porous glasses (Vycor and a silica xerogel). ac heat-capacity measurements show broadened latent-heat peaks associated with both freezing and melting at temperatures substantially below the bulk melting temperatures. Thermal cycling shows pronounced hysteresis, with melting occurring at a higher temperature than freezing. Also, the latent heat of freezing appears to be much smaller than that of melting. The hysteresis in the argon-Vycor system was studied in detail using high-resolution ultrasonic techniques which directly probe the shear modulus of the material in the pores. We found that the onset of freezing is extremely sharp, despite the random pore geometry, and that freezing continues over a range of temperatures. The freezing process is extremely irreversible, in the sense that, once the solid appears, subsequent warming does not cause it to melt until a much higher temperature. This is true even if only a small fraction of the fluid is initially frozen. The melting branch of the hysteresis loop is more nearly reversible. In order to correctly measure the latent heat of freezing in the presence of such hysteresis, a technique should be used in which cooling is performed monotonically, for example, thermal relaxation or differential scanning calorimetry.

## INTRODUCTION

We report here the results of a combined heat-capacity and ultrasonic study of the freezing and melting of simple fluids confined in porous glasses. The heat-capacity measurements were made on several fluids confined either in Vycor glass or in a silica xerogel with similar pore sizes. Relatively broad latent-heat peaks were observed both during cooling (freezing) and during warming (melting). Freezing temperatures were significantly below the bulk values. Melting occurred at higher temperatures, but still below the bulk melting points. Surprisingly, the areas under the cooling heat-capacity peaks, usually interpreted as latent heats associated with freezing, were considerably smaller than those measured during melting, with no indication of where the missing energy went. To clarify this behavior, we made a detailed ultrasonic study of the hysteresis between the freezing and melting of argon in Vycor glass. We found that the onset of solidification in the pores of Vycor remains extremely sharp, but that freezing continues over a range of temperature. Furthermore, the freezing is highly irreversible. Any solid which forms, even very small amounts, remains frozen until warmed well above the temperature at which freezing began. Melting is complete at a well-defined temperature roughly halfway between the onset of freezing and the bulk melting temperature. In contrast to freezing, melting is nearly reversible. That is, when the solid is partially melted by warming, it appears to immediately refreeze when the sample is recooled. Only when the solid has completely melted does the original freezing behavior reappear. Below, we present our results and discuss the interpretation of the heat-capacity data in light of the hysteresis between freezing and melting seen in the ultrasonic measurements.

When materials are confined within small pores, their properties may be substantially modified. Phase transitions in particular can be strongly affected by the restriction to finite size, by interactions with the pore surfaces, and by the disorder introduced by the porous medium. Recently, the superfluid transition,[1] the liquid-vapor critical point[2] and binary-fluid phase separation[3] have all

 

been intensively studied in various confining geometries. Despite the random nature of the porous media used, sharp, well-defined critical behavior is often observed, but with transition temperatures, critical exponents, and time dependence quite different from the corresponding bulk systems.

First-order phase transitions have not been studied in the same detail, but there have been a number of experiments on the melting and freezing of confined fluids. These include thermal expansion,[4] heat-capacity,[5–11] ultrasonic,[12] pressure,[13–15] torsional-oscillator,[16] NMR,[17] light-scattering,[18] and neutron-scattering[19,20] measurements in a number of porous and granular media. The results have several common features which appear to be characteristic of first-order transitions in small pores. The freezing and melting transitions are broadened and occur at temperatures below the bulk melting point. This depression of the transition temperatures is inversely proportional to the pore size and is not simply supercooling, since it occurs for melting as well as freezing. Also, there is no indication of the time dependence which would be expected if nucleation kinetics were important. Pronounced hysteresis is observed, with melting occurring at a higher temperature than freezing.

Several of the experiments[7,8,10,11,13] also found latent heats or volume changes considerably smaller than those associated with bulk melting. This could reflect inherently smaller latent heats for melting in finite-size systems, or it could mean that only part of the material in the pores participates in freezing and melting, as might happen if, for example, there was an amorphous surface layer. In one experiment,[8] melting of hydrogen confined in the pores of Vycor was accompanied by an entropy change about half as large as bulk hydrogen. The authors speculated that liquid hydrogen might remain even at very low temperature and were able to fit their heat-capacity data at lower temperatures by a rotonlike expression. Another experiment[7] was similarly interpreted as meaning that much of the helium in Vycor pores remains liquid, even at the lowest temperatures and highest pressures.

Although most of the latent-heat measurements involved melting, a few also measured the latent heat of freezing.[5,6,8] As well as occurring at a lower temperature, the latent-heat peak due to freezing is much narrower than that due to melting. More surprisingly, in several of these experiments the latent heat of freezing is smaller than the latent heat of melting, apparently violating energy conservation.

Some of these features can be understood in a simple model of freezing which includes the effect of the interface between liquid and solid. This surface has an associated free energy which, for example, is important in determining how far a bulk fluid can be supercooled before solid nucleates. In bulk systems, once a critical nucleus forms, it immediately expands until all the fluid is frozen, since the gain in volume free energy more than compensates for the cost in surface free energy. In a porous medium, however, the situation is different. If the solid phase does not "wet" the pore surface, then freezing must begin in the center of a pore, but the solid nucleus cannot be larger than a pore.

If a spherical pore of radius $r$ freezes at a temperature $\Delta T$ below the bulk transition temperature $T_0$, the surface and volume contributions add to give a total free-energy change

$$\Delta G = 4\pi r^2 \sigma_{\mathrm{LS}} - \frac{4}{3}\pi r^3 \frac{l_F \Delta T}{v_S T_0} , \tag{1}$$

where $\sigma_{\mathrm{LS}}$ is the liquid-solid interfacial free energy, $l_F$ is the latent heat of freezing, and $v_s$ is the solid's molar volume. Freezing then occurs at the temperature where this free-energy change first becomes negative. This "geometric-freezing" model predicts the fluid will solidify at an undercooling

$$\Delta T = \frac{3\sigma_{\mathrm{LS}} v_S T_0}{l_F r} . \tag{2}$$

In the case of helium, where it is known that the solid phase does not wet most surfaces and where the solid-liquid interfacial energy has been directly measured, this model gives semiquantitative agreement with the freezing-point depression observed in the pores of Vycor.[12,13]

In this model, the sharpness of the onset of freezing and the width of the transition are reflections of the distribution of pore sizes in the medium. However, the model itself does not offer any explanation of the hysteresis between freezing and melting; nor does it explain why the latent heats and volume changes should be different from the bulk values. It is possible to introduce hysteresis in such models by considering interconnected pores or pores with different shapes, but it is difficult to relate these models to the complex and random geometries of the porous media studied to date.

We have used both heat-capacity and ultrasonic measurements to study the freezing and melting of simple fluids in small pores. For the heat capacity, we made measurements on hydrogen, neon, oxygen, and argon. Two porous media were used, Vycor glass[21] and a silica xerogel.[22] Vycor glass has been used in much of the previous work on freezing in porous media. It is made by a spinodal decomposition and leaching process which results in a completely interconnected pore network with a fairly narrow pore-size distribution. Its pores are small, about 3.6 nm, and so the undercooling and hysteresis are pronounced. The xerogel had comparable pore sizes, but was formed by a sol-gel process and had a somewhat different microstructure. Qualitatively similar freezing and melting behavior was observed in all cases. In the case of oxygen, the heat-capacity data showed latent-heat peaks associated both with freezing and with the structural phase transition which occurs at lower temperatures.

Although these measurements provide fundamental thermodynamic information, they have limited sensitivity. Also, in the hysteretic region between freezing and melting, we would like to have a technique which directly probes the amount of solid present, in contrast to heat-capacity measurements which can only infer the existence

of solid from the latent heat when it melts or freezes. Since any solid in the pores contributes directly to the system's shear modulus, ultrasonic measurements can provide a very sensitive probe of freezing and melting to complement the specific-heat measurements. Previous experiments[12] have shown Vycor to be an excellent substrate for ultrasonic experiments, and in contrast to the silica xerogel, samples were available with suitable dimensions. Accordingly, we have made a detailed ultrasonic study of the freezing and melting of argon in Vycor.

## EXPERIMENTAL DETAILS

The calorimetric measurements were made using an ac technique[23] because of the high precision and fast turn around time the method offers. In this technique, a thermometer and an electrical heater are mounted on a sample which is then coupled to a temperature bath via a weak thermal link. When an oscillating (ac) heat input is supplied, the sample temperature oscillates about an average temperature determined by the heater power and the thermal conductivity of the thermal link to the bath. If the heat input's ac period is long compared to the internal thermal time constant of the sample but short compared to the time for the sample to come into equilibrium with the external bath, then the amplitude of the sample's temperature oscillation is inversely proportional to its heat capacity. For glasses such as Vycor and silica xerogel, the necessary short internal relaxation times can be achieved by making the samples in the form of thin disks, as described below. In our experiments, the frequency of the ac heat input was about 0.1 Hz, compared to internal and external relaxation times of about 1 and 100 s, respectively.

The silica gel samples came in the form of irregular lumps approximately 5 mm in diameter. One of these was sanded to a thickness of 1 mm with two parallel flat surfaces. It was then encapsulated with a thin (approximately 0.25 mm) layer of Stycast 2850 epoxy. A 0.25-mm-i.d. copper-nickel capillary was potted into the epoxy and served as a fill line as well as providing the weak thermal link to the bath (a platform whose temperature was regulated to within 5 mK). A film of germanium-gold alloy (18 wt. % gold) was evaporated on a thin sapphire disk to serve as the thermometer. The Ge-Au thermometer was calibrated against a silicon diode as well as the bulk triple-point signatures provided by the excess bulk fluids in the filling capillary. The Vycor sample was prepared in a similar manner. The sample was cut from a $\frac{1}{2}$-in.-diam rod using a diamond impregnated wire saw. This disk was sanded to 0.23 mm in thickness before coating with about 0.25 mm of Stycast 1266 epoxy. A 0.10-mm-i.d. copper-nickel capillary was used as the fill line. The thermometer for this sample was an Allen-Bradley carbon resistor.

The Vycor glass used in the calorimetric measurements was cleaned by boiling in 30% $H_2O_2$ for 30 min followed by boiling in distilled water for 30 min. It was then dried in a chamber constantly flushed with extra-dry grade nitrogen. When dry, Vycor has a porosity $\phi$ of about 28% and a specific surface area of about 100 $m^2/g$, corresponding to an effective cylindrical pore radius of 3.6 nm. Its pores have a rather narrow size distribution, with 96% of the pore diameters lying within $\pm 0.6$ nm of the average diameter. The xerogel sample had a porosity of about 60% and, from a Brunnauer-Emmett-Teller (B.E.T.) adsorption isotherm measurement, an effective cylindrical pore radius of about 5.1 nm. Mercury intrusion porosimetry indicated a pore-size distribution at least as narrow as that of Vycor glass.

Before filling the porous glasses with a fluid, the heat capacity of the empty cell (glass, epoxy, thermometer, and heater) was measured. This addendum heat capacity varied smoothly with temperature and could be fit to a polynomial which was then subtracted from the heat capacities measured in later runs. This addendum correction was always less than about 30% of the total heat capacity. To begin each measurement, the sample cell was slightly overfilled at a temperature about 2 K above the bulk triple point. This ensured that the sample pores remained completely filled for the entire temperature range studied. The heat capacity was then measured with the calorimeter cooling down or warming up. The temperature was varied by controlling the temperature of the bath. After a change in the bath temperature, the sample temperature stabilized in a couple of minutes and the heat-capacity signal was monitored for 10 min until it became steady. It was then averaged for about 20 min. The procedure was rapid enough that a complete thermal cycle typically took less than 24 h.

The Vycor used in the ultrasonic experiments was in the form of a cyclindrical rod about 0.3 cm in diameter. This was cut into pieces about 1 cm long whose ends were polished flat and parallel. These samples were cleaned by heating at 80 °C in a 30% hydrogen peroxide solution for 1 h, followed by rinsing in methanol and distilled water for several hours. After air drying, $LiNbO_3$ shear transducers with fundamental frequency 20 MHz were attached to the ends using Tra-Bond BA2151 epoxy. The samples were then sealed into a copper cell (volume about 10 $cm^3$). The cell was attached by a fairly weak thermal link (a brass rod) to the cold stage of a helium closed-cycle refrigerator. A radiation shield at about 75 K minimized thermal gradients in the apparatus. Once mounted, the cell was flushed with helium gas and evacuated for several hours at room temperature. The cell was then cooled to 87.5 K, and an argon adsorption isotherm was obtained *in situ*. This gave a specific surface area of 96 $m^2/g$. Together with the measured porosity ($\phi = 29\%$), this gives an effective cylindrical pore radius $r \approx 3.9$ nm, somewhat larger than the neck radius of $\approx 1.9$ nm determined by mercury intrusion porosimetry on a sample from the same batch. After the adsorption isotherm showed that the sample was completely filled, enough argon was admitted to the cell to ensure that the pores remained filled as the cell was cooled.

The temperature of the ultrasonic cell was measured using a calibrated carbon glass sensor and a digital resistance bridge. This allowed the temperature to be controlled to within 0.02 K in the temperature range of the experiments. The ultrasonic velocity $v$ and attenuation $\alpha$

were measured simultaneously at each temperature with a resolution of $\Delta v/v_0 \approx 10^{-6}$ and $\Delta\alpha \approx 0.005$ dB/cm, respectively. After the temperature had stabilized at each point, about 15 min were required to take data over the complete frequency range (typically about six frequencies from 8 to 22.5 MHz). As a result, cooling and warming rates were slow, with several days required for each temperature sweep.

## RESULTS

We begin by presenting the results of the calorimetric measurements. Figure 1 shows the heat capacities of hydrogen and neon in the pores of the Vycor calorimeter. The solid symbols are the data taken during cooling from temperatures above the bulk triple points, and the open symbols are the data during warming from the lowest temperatures. The most obvious features are the large heat-capacity peaks seen during warming. These represent the latent heats associated with melting the hydrogen or neon in the pores. It is also striking how little latent heat is observed during cooling (the freezing peak near 10.7 K is barely visible in the hydrogen data of Fig. 1). Both the melting and freezing latent-heat peaks occur below the bulk triple-point temperatures (13.8 K for $H_2$ 24.6 K for Ne), with melting occurring at higher temperatures than freezing.

The results for oxygen and argon contained in the pores of the xerogel calorimeter were qualitatively similar. Figure 2 shows the results for oxygen, which obviously undergoes two first-order transitions in the temperature range studied. Upon cooling (solid symbols), it first froze at about 47.5 K and then went through a solid-solid phase transition at 36 K (the triple-point and $\gamma$-$\beta$ transition temperatures are 54.4 and 44 K in bulk oxygen).

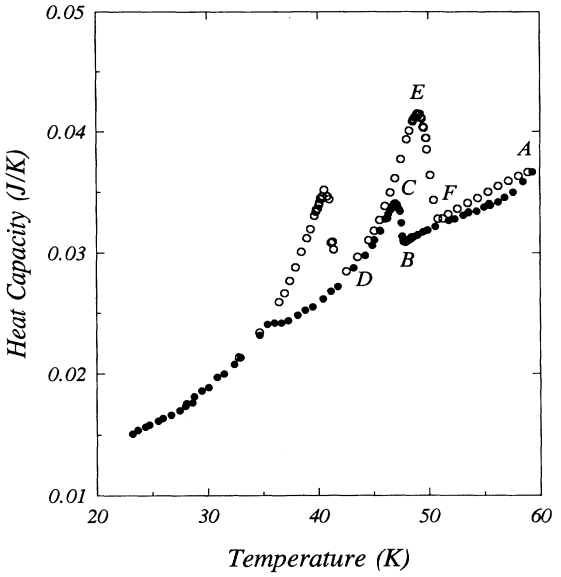


FIG. 2. Heat capacity for oxygen confined in the pores of a silica xerogel. Data taken during cooling (solid circles) and during warming (open circles). Points labeled $A-F$ are discussed in the text.

Both of these transitions in bulk $O_2$ involve substantial latent heats and volume changes, and their heat-capacity signatures in Fig. 2 are comparable. The two transitions show similar hysteretic behavior, with higher transition temperatures and larger latent-heat peaks during warming (open symbols) than during cooling. Figure 3 presents the results for argon in the same xerogel. Unfortunately, the limited sensitivity of the thermometer in

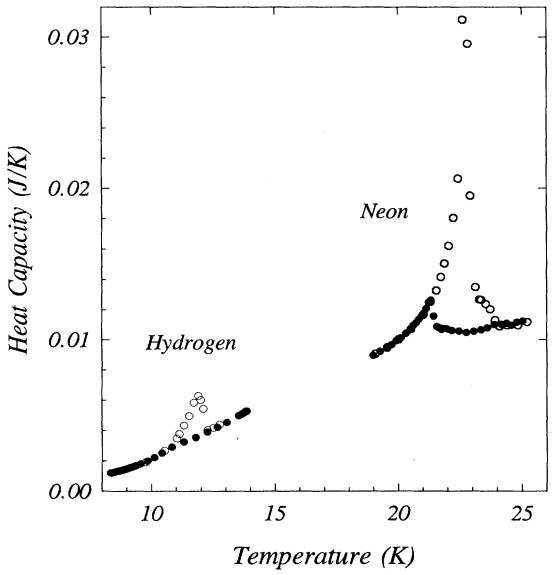


FIG. 1. Heat capacity for hydrogen and neon confined in the pores of Vycor glass. Solid circles are data taken during cooling, and open circles are data taken during warming.

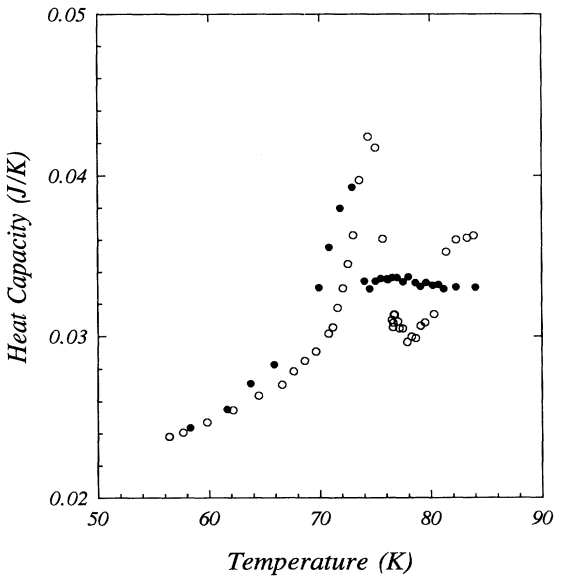


FIG. 3. Heat capacity for argon in xerogel pores. Data taken during cooling (solid circles) and during warming (open circles).

this temperature range results in considerable scatter in the data. However, the behavior is qualitatively similar to the other cases. A summary of the transition temperatures determined from the heat-capacity peaks is given in Table I.

To examine the freezing-melting hysteresis in more detail, we now turn to the ultrasonic measurements on argon in Vycor. Since the ultrasonic wavelengths are much larger than the Vycor pores, such a system behaves as a single isotropic medium characterized by its total density $\rho$ and its shear modulus $\mu$. This is true even when the argon is liquid, since in pores as small as those of Vycor, the fluid is dragged along with the solid matrix by its viscosity. The total density is $\rho=\rho_{\text{Vycor}}+\phi\rho_{\text{Ar}}$, where $\rho_{\text{Vycor}}$ is the density of the empty Vycor and $\rho_{\text{Ar}}$ is the density of the argon. When the argon in the pores is liquid, the system's shear modulus is just that of empty Vycor, $\mu_{\text{Vycor}}$. Once the argon freezes, however, the system's shear modulus increases to $\mu=\mu_{\text{Vycor}}+\Delta\mu_{\text{Ar}}$. The contribution of the solid argon to the shear modulus, $\Delta\mu_{\text{Ar}}$, can be roughly estimated as[12]

$$\Delta\mu_{\text{Ar}}=\frac{1}{\phi}\left[1-\frac{\mu_{\text{Vycor}}}{\mu_s}\right]^2\mu_{\text{Ar}}\ , \tag{3}$$

where $\mu_s$ and $\mu_{\text{Ar}}$ are the shear moduli of solid (nonporous) Vycor and of solid argon, respectively. Using the values $\phi=0.29$, $\mu_{\text{Vycor}}=7.5\times10^9$ Pa, $\mu_s=2.7\times10^{10}$ Pa, and $\mu_{\text{Ar}}=8\times10^9$ Pa, Eq. (3) predicts a modulus change $\Delta\mu_{\text{Ar}}\approx1.5\times10^9$ Pa. Since the transverse sound velocity is simply given by

$$v=\left[\frac{\mu}{\rho}\right]^{1/2}=\left[\frac{\mu_{\text{Vycor}}+\Delta\mu_{\text{Ar}}}{\rho_{\text{Vycor}}+\phi\rho_{\text{Ar}}}\right]^{1/2}\ , \tag{4}$$

the expected signature of freezing in the pores is an increase of roughly 10% in the transverse sound velocity, providing a sensitive and direct way of monitoring the freezing process.

Figure 4 shows the transverse sound velocity (solid symbols, left axis) and attenuation (open symbols, right axis) at a frequency of 14 MHz during the cooling of argon-filled Vycor glass. Nothing happens at the bulk freezing point ($T_b=84$ K), but a sudden increase in both the sound speed and attenuation at $T_f=75.55$ K signals the onset of freezing in the pores. The slight decrease in the sound velocity as the temperature is lowered from 87 K to the freezing point $T_f$ is simply a density effect due

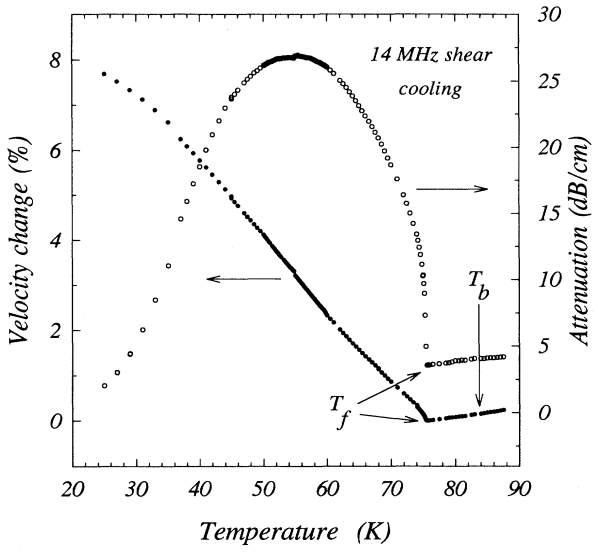


FIG. 4. Velocity (solid symbols, left axis) and attenuation (open symbols, right axis) of 14-MHz transverse ultrasonic waves in argon-filled Vycor glass. Data taken during cooling. Onset of freezing in the pores is marked by $T_f$; bulk freezing point is marked by $T_b$.

to thermal contraction of the liquid argon in the pores. When the sample is cooled below $T_f$, the velocity continues to increase down to at least 25 K. The total change, nearly 8%, is comparable to that expected when the argon freezes completely. It would thus appear that freezing occurs over a temperature range much wider than the heat-capacity results would indicate, with some liquid remaining at temperatures as low as 25 K. However, for the case of helium freezing in Vycor,[12] a similar gradual increase in the sound velocity has been explained in terms of thermally activated motion of vacancies which relaxes the stresses in the solid helium. We believe that this also occurs in argon and that the fluid is completely frozen within a few degrees of $T_f$.

During the passage of a transverse sound wave, pores are distorted and local stresses are set up in the argon. When the argon is liquid, viscous flow within each pore relaxes these stresses very rapidly. Within a small pore, the stress is relaxed in a time of order $\eta/K$, where $\eta$ is the liquid's viscosity and K is its bulk modulus. For argon ($\eta\approx2.7\times10^{-4}$ Pa s and $K\approx1.0\times10^9$ Pa), this time is less than $10^{-12}$ s, a small fraction of the ultrasonic period, and so the liquid makes a negligible contribution to the shear modulus. When the argon is frozen, viscous flow is no longer possible and stresses within a pore relax much more slowly. The most important stress relaxation mechanism in small crystals near their melting point is via "Nabarro-Herring creep."[12,24] This involves the diffusion of thermally activated vacancies along the stress gradient. In pores as small as those of Vycor, vacancies can diffuse from one side of a pore to the other very quickly. The time constant for relaxation of stress in a crystal of size $L$ is given by

TABLE I. Temperatures of the heat-capacity peaks for various fluids in porous glasses.

| Transition | Porous glass | Cooling peak (K) | Warming peak (K) | Bulk (K) |
|---|---|---|---|---|
| $H_2$ solid-liquid | Vycor | 10.7 | 11.9 | 13.8 |
| Ne solid-liquid | Vycor | 21.3 | 22.7 | 24.6 |
| $O_2$ solid-liquid | xerogel | 47.5 | 49.1 | 54.4 |
| $O_2$ solid-solid | xerogel | 36.0 | 40.5 | 43.8 |
| Ar solid-liquid | xerogel | 72.3 | 74.8 | 84.0 |

$$\tau=\frac{k_B T L^2}{2\alpha\mu_{\mathrm{Ar}} V D}\ , \tag{5}$$

where $\alpha$ is a shape-dependent numerical factor ($\alpha\approx 16$ for spherical grains), $V$ is the atomic volume ($V\approx 4\times 10^{-29}$ m$^3$), and $\mu_{\mathrm{Ar}}$ is the shear modulus. The self-diffusion coefficient of solid argon, $D$, has the usual form

$$D=D_0 e^{-E_v/k_B T}\ , \tag{6}$$

where, for bulk argon,[25] $D_0\approx 0.035$ m$^2$/s and $E_v$, the activation energy for vacancy diffusion, is about 2000 K.

Since in our system the stresses occur on a length scale of the pore size, we use $L=3.9$ nm and find that, at the bulk melting temperature, stresses within a pore would relax via vacancy diffusion in a time $\tau\approx 8\times 10^{-10}$ s. This is less than the period of the ultrasonic waves so that, near melting, solid argon will behave more like a highly viscous liquid. The full contribution $\Delta\mu_{\mathrm{Ar}}$ will not be observed until the relaxation time becomes much longer than the sound period. If the angular frequency of the sound wave is $\omega$, then the crossover (where the solid argon's contribution to the system modulus is one-half of its limiting low-temperature value) occurs at $\omega\tau=1$. At a sound frequency of 14 MHz, using the bulk parameters above, this occurs at a temperature about 15 K below bulk freezing. Of course, when argon is confined in pores as small as those of Vycor, properties such as vacancy diffusion rates may be somewhat different from bulk values. In any case, we expect that the sound velocity will begin to increase as soon as some of the argon freezes, but that the full modulus contribution of the solid argon will only be observed at temperatures well below the freezing point.

The velocity change in a relaxation process is always accompanied by dissipation, with the maximum attenuation occurring when $\omega\tau=1$. The ultrasonic attenuation shown in Fig. 4 has a large peak at about 55 K. If this is the crossover temperature where $\omega\tau=1$, then half of the total sound-velocity increase should have occurred. Figure 4 shows this to be the case, confirming that we are observing the effects of a thermally activated stress-relaxation process. In addition, ultrasonic measurements made over a limited frequency range (8–22 MHz) showed the expected relaxation behavior, with the velocity increase and attenuation peak shifting to higher temperature as the sound frequency was increased.

Since both the ultrasonic velocity and the attenuation are sensitive to the presence of solid argon in the pores of Vycor, we have used them to study the freezing and melting behavior in some detail. Figure 5 shows the velocity and attenuation near the freezing transition on an expanded scale. Note how sharp the onset of freezing is; its rounding is at most 0.05 K, most of which is due to the stability of the temperature controller (the temperature fluctuated about 0.02 K). The onset temperature appears to be intrinsic in the sense that it does not depend on the cooling rate. The sample can be cooled to within 0.1 K of the transition and held there for many hours without any freezing occurring. If, on the other hand, it is cooled

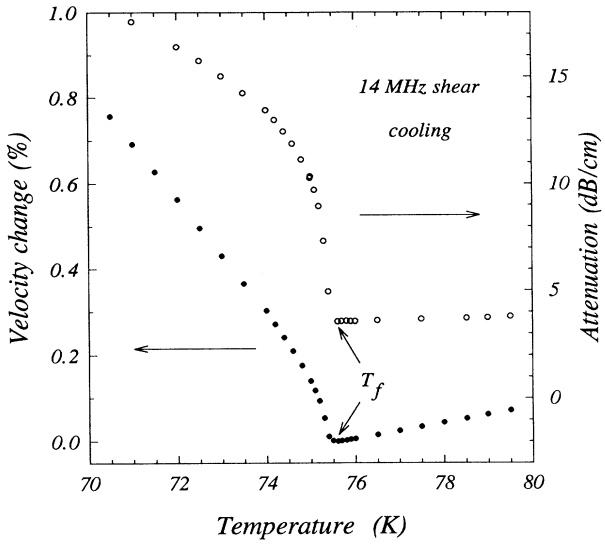


FIG. 5. Sound velocity (solid symbols, left axis) and attenuation (open symbols, right axis) in argon-filled Vycor close to the onset of freezing.

0.1 K below the onset temperature, the sound velocity and attenuation increase immediately and then stabilize, indicating that freezing occurs within seconds. Also, the amount which freezes depends only on the temperature; waiting for hours at a fixed temperature below the onset temperature does not result in any further changes.

After cooling the sample well below the freezing point, we made measurements while warming. Figures 6 and 7

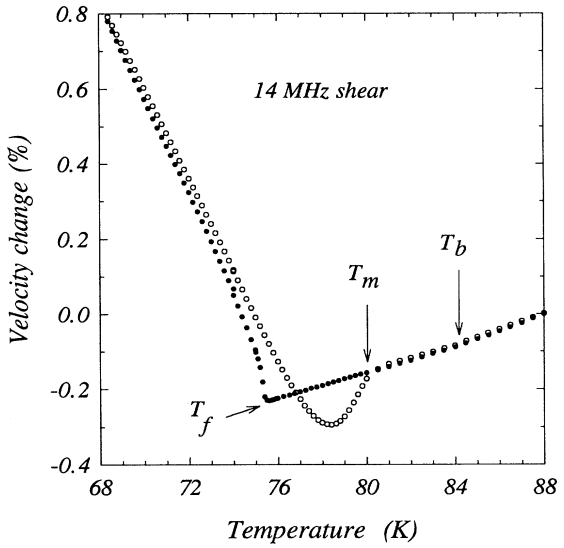


FIG. 6. Sound velocity in argon-filled Vycor showing the hysteresis between freezing and melting. Solid circles are data taken during cooling, and open circles are data taken during warming. Onset of freezing is marked by $T_f$, completion of melting is marked by $T_m$, and bulk melting point is marked by $T_b$.

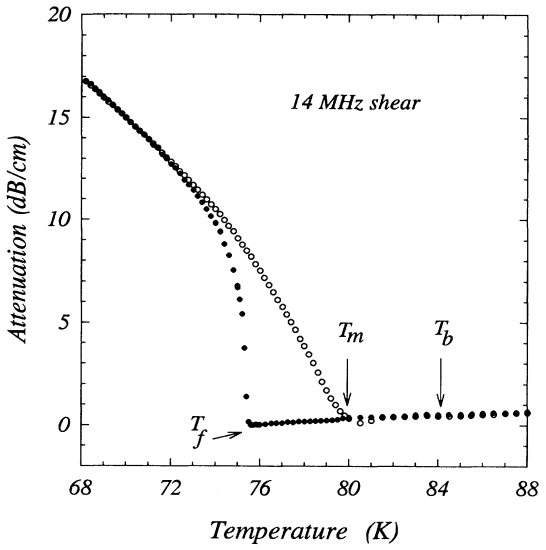


FIG. 7. Sound attenuation coresponding to the sound velocity of Fig. 6.

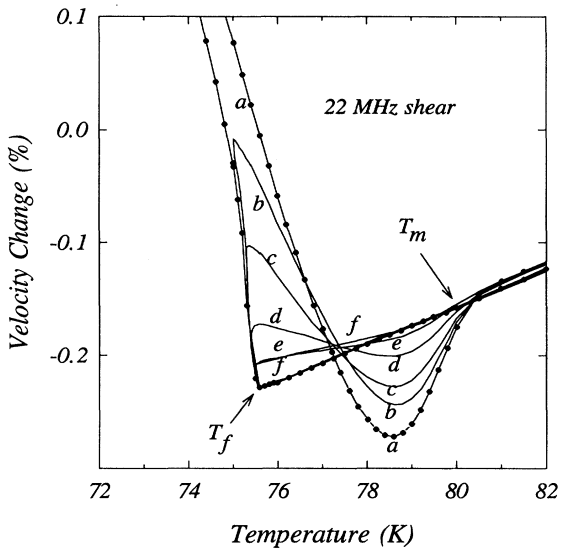


FIG. 8. Velocity of 22-MHz transverse sound in argon-filled Vycor. The curves labeled $a-f$ are hysteresis loops with minimum temperatures successively closer to the onset of freezing at $T_f=75.55$ K. The minimum temperatures are 68 K ($a$), 75.0 K ($b$), 75.3 K ($c$), 75.4 K ($d$), 75.45 K ($e$), and 75.52 K ($f$).

show velocity and attenuation data from a typical thermal cycle. Below about 72 K, the warming and cooling data are very similar. At higher temperatures, however, the warming curves are quite different and only rejoin the cooling curves at a temperature $T_m=80$ K, which we identify as the completion of melting in the pores. If a sample which has been warmed above $T_m$ is then cooled again, the entire freezing-melting hysteresis loop can be accurately reproduced. One interesting feature of Fig. 6 is the region between $T_f$ and $T_m$ where the sound velocity during warming dips below that during cooling. This is surprising, since this is the region where during warming there is some solid present to increase the shear modulus, but only liquid during cooling. Therefore, the total density must be larger during warming. This can only occur if there is mass transport from the bulk argon outside the sample as the fluid in the pores freezes and contracts. During the initial stages of freezing, this can occur easily via fluid flow through the pores to the surface. However, even later, when the paths to the surface are blocked by frozen argon, vacancy diffusion through the solid is rapid enough to provide the necessary mass transport.[12]

We next made a number of measurements where cooling was stopped at different temperatures below the onset of freezing to see what happens when only part of the argon is initially frozen. The results are shown in Figs. 8 and 9. We began each cycle above the bulk freezing temperature to ensure that there was no solid argon present. We then cooled to some temperature below $T_f$ (75.55 K), stopped, and warmed the sample until all the argon had melted. This procedure was then repeated, each time stopping at a temperature closer to $T_f$. The paths in Fig. 8 labeled $a-f$ correspond to cycles in which the lowest temperatures were 68, 75.0, 75.3, 75.4, 75.45 and 75.52 K, respectively. The first curve $a$ is essentially the same as the curves obtained when the sample was cooled to the lowest temperatures (below 25 K) and, we believe, corresponds to the case where all the argon is frozen at the lowest temperature. The smaller changes in velocity and attenuation in the other curves correspond to smaller fractions of solid argon at the minimum temperatures. In curve $f$, for example, the velocity increase due to freezing is only a few percent of that when all the argon is frozen (curve $a$). No matter how close to the onset of freezing we stopped cooling, the velocity during warming fol-

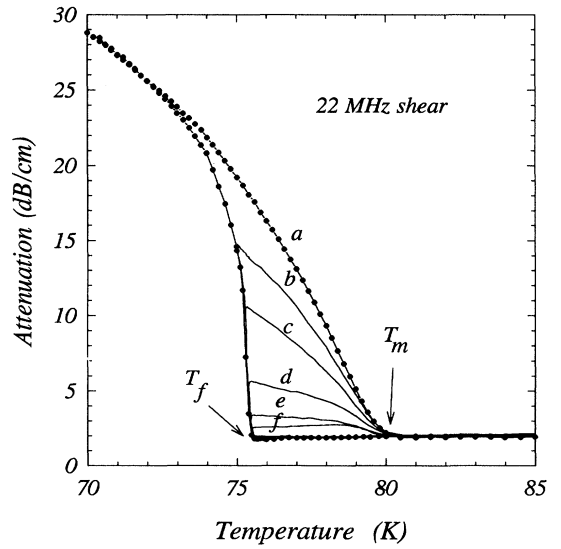


FIG. 9. Attenuation data corresponding to the sound velocities of Fig. 8.

lowed a path quite different from that during cooling. From the slopes of the cooling and warming curves near the minimum temperature, it is clear that when the Vycor is rewarmed, for example, up to $T_f$, very little of the frozen argon remelts. In fact, none of the warming curves rejoin the cooling curve until the temperature reaches $T_m$. This implies that freezing in the argon-Vycor system is highly irreversible; no matter how little of the argon in the pores is initially frozen, it must be warmed all the way to $T_m$ before melting is complete.

We also looked at the warming branch of the hysteresis loop. Figure 10 shows the attenuation when the system was cooled from an initial temperature ($A$) where all the argon was liquid, past the onset of freezing ($B$), to a temperature ($C=75.4$ K), where a fraction of the argon was frozen. We then warmed the sample to a higher temperature ($D=77.0$ K), stopped, and then recooled. Upon cooling from point $D$, the sound attenuation (and velocity) approximately retraced their warming path back to the minimum temperature reached in the initial cooldown (point $E$). When the sample was further cooled below $E$, the velocity immediately began to increase more rapidly, along the path it would have followed had we continued cooling from $C$ to $F$ without the detour to $D$ and back. These results indicate that any argon which melted during warming from $C$ to $D$ refroze nearly reversibly upon subsequent cooling to $E$. Also, the argon initially frozen at $C$ is stable in the sense that no more will freeze unless the temperature is reduced below $C$. Since the warming (melting) branch of the hysteresis loop appears to be more nearly reversible than the cooling (freezing) branch, we looked at it in more detail. Figure 10 also shows the attenuation for two warming-cooling cycles starting from 74 K (point $F$). First, we warmed to 76 K ($G$), stopped, and recooled to $F$. Then we repeated the process, this time stopping at 78 K ($H$) before cooling back to $F$. We see that warming and cooling along this melting branch of the hysteresis loop is nearly reversible in this temperature range. However, if we warm above $T_m$, then the original hysteresis loop should be reproduced, since we believe that $T_m$ represents the completion of melting in the pores. In Fig. 11 we show the results of several cycles in which we warmed from 74 K ($F$) to a temperature near $T_m$ before cooling back to point $F$. Warming from $F$ gave the same curve (labeled $a$) each time, but the curves corresponding to cooling differed. The curves labeled $b$, $c$, and $d$ correspond to recooling after stopping at temperatures of 79.5 K ($I$), 79.75 K ($J$), and 81 K ($K$). We see that the hysteresis increases fairly abruptly when the maximum temperature is close to $T_m$.

Although we did not study the hysteretic behavior of the heat capacity in as much detail, it was consistent with the ultrasonic data. For example, in the oxygen-xerogel system of Fig. 2, if the sample was cooled slowly from point $A$ above the bulk triple point to the onset of the freezing (point $B$), the heat capacity was reversible. In other words, if the cooling was stopped somewhere in the temperature range $A-B$ and subsequently warmed up, the heat capacity during warming would retrace the cooling data. However, if the minimum temperature was below point $B$, hysteresis set in. For example, the open circles correspond to warming from about 23 K. We found that if the minimum temperature was anywhere below the maximum of the freezing peak (point $C$), then the heat capacity during subsequent warming followed

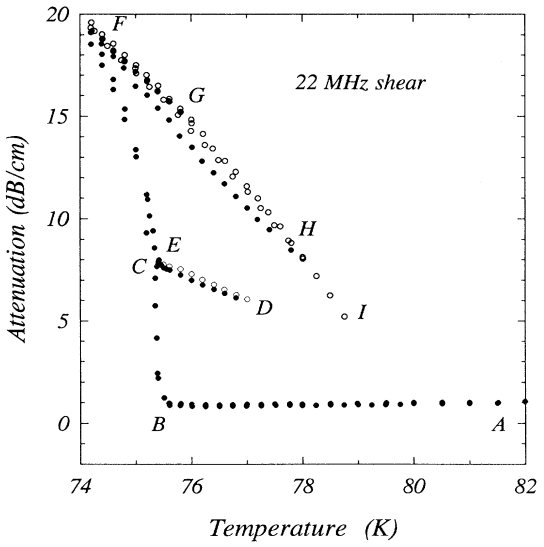


FIG. 10. Sound attenuation in argon-filled Vycor. Cooling began at $A$ and continued to $C$. The sample was next warmed to $D$, cooled back to $E$, and then to $F$. The sample was then cycled back and forth along the warming branch of the hysteresis loop. ($F$ to $G$ and back, then $F$ to $H$ and back, finally to $I$). Solid symbols are data taken during cooling, open symbols taken during warming.

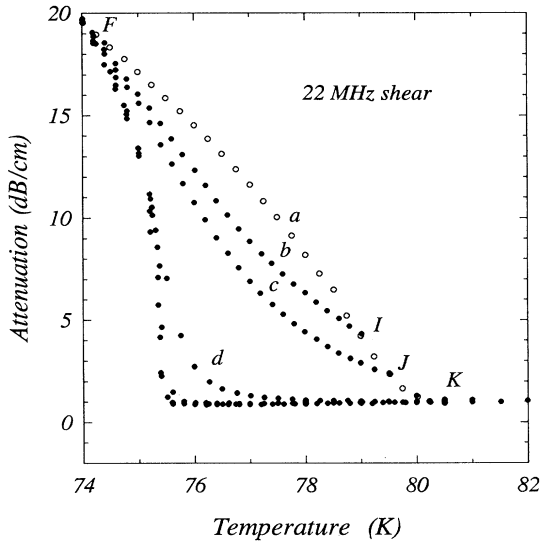


FIG. 11. Sound attenuation in argon-filled Vycor. The sample was initially cooled to $F$ along the lower curve then warmed along curve a (open circles) to successively higher temperatures of 79.5 K (point $I$, cooling curve $b$), 79.75 K (point $J$, cooling curve $c$), and 81 K (point $K$, cooling curve $d$).

the same path (e.g., that shown as open circles). However, if the cooling was stopped somewhere between point $B$ and $C$ and then warmed, the heat capacity would follow a path intermediate between the cooling and warming branches shown in Fig. 2. Similar behavior was observed during warming. If the warming was stopped between points $D$ and $E$ and cooled back down, the heat capacity would follow the warm-up branch reversibly. Once the temperature was warmed above point $E$, the hysteresis would set in again. If the system was warmed above point $F$, cooling down would reproduce the original cooling results (solid circles), while stopping between points $E$ and $F$ gave cooling heat capacities intermediate between the two branches. Points $B$ and $F$ in Fig. 2 are thus the analogs of the points marked $T_f$ and $T_m$ in the ultrasonic data.

## DISCUSSION

The latent heat associated with a phase transition is usually calculated as the area under a heat-capacity curve after subtracting the background temperature dependence well away from the transition. Our data of Figs. 1–3 then appear to imply latent heats which are much smaller for freezing than for melting. However, in the presence of hysteresis, heat-capacity measurements must be interpreted very carefully. As pointed out by Tell and Maris,[5] techniques such as adiabatic heat-pulse calorimetry actually measure the temperature *rise* due to an *input* of heat, even when the sample is being cooled between data points. From our ultrasonic measurements, it is clear that such a measurement would miss much of the latent heat associated with freezing, since the freezing would occur when the temperature was initially reduced and little of the new solid would melt during the small temperature rise associated with the heat-pulse input. In principle, the adiabatic heat-pulse technique should still give the correct latent heat during melting, although in the presence of hysteresis it may be important to avoid overshoots when the temperature is changed. The ac calorimetric technique used in our measurements suffers from essentially the same problems, since it measures only the latent heat associated with material which melts and freezes reversibly during the small temperature oscillation. From our ultrasonic studies of the hysteresis, we expect this to be fairly accurate on most of the warming branch, except near the completion of melting. During cooling, on the other hand, very little of the newly formed solid melts during the small temperature oscillation, and so most of the latent heat of freezing will be missed, as observed in Figs. 1–3. Thus our heat-capacity curves give an underestimate of the latent heats, particularly during freezing, so that energy conservation is not threatened.

The only way to ensure that no latent heat is missed is to cool or heat monotonically, as is done in differential scanning calorimetry. In fact, the heat-capacity measurements of Torii, and Maris and Seidel[6] used a thermal-relaxation method in which the sample (hydrogen in Vycor) was cooled monotonically. In contrast to our results shown in Fig. 1, they did observe a substantial heat-capacity peak associated with freezing, corresponding to a latent heat approximately equal to that of bulk hydrogen.

Despite the problems hysteresis causes when an ac technique is used to measure the heat capacity, the data of Figs. 1–3 clearly illustrate the depression of the freezing and melting transition temperatures in small pores. The temperatures of the heat-capacity peaks given in Table I agree quite well with those measured by other workers.[5,6,8,19] It is interesting to note here that the fractional shifts in freezing temperatures ($\Delta T/T_0$) are roughly the same (about 13%) for neon in Vycor as for oxygen and argon in the xerogel. However, the hydrogen in Vycor had a much larger fractional shift of around 22%. Such a high susceptibility to geometric cooling may help in the search for superfluidity in supercooled molecular hydrogen.

The fact that the onset of freezing at $T_f$ does not depend on the cooling rate indicates that freezing is controlled by the pore geometry and not by nucleation kinetics. It appears that, by halting the cooling at a temperature close to $T_f$, it is possible to have a stable state in which an arbitrarily small fraction of argon is frozen. If supercooling were occurring, one would expect freezing, once initiated, to continue until a finite fraction was solid. This may be prevented by the pore geometry, since small necks between pores would stop the solid-liquid interface from propagating from one pore to another, so that each pore freezes independently.

Despite the sharpness of the onset, both the width of the latent-heat peaks and the hysteresis loops in the ultrasonic data (Figs. 8 and 9) indicate that freezing proceeds over a range of temperatures. Since in the geometric-freezing model the depression of the freezing point is inversely proportional to the pore size, Adams *et al.*[13] have described such freezing measurements as providing a "spectrometer of pore size." The very sharp onset of freezing seen in the ultrasonic data (e.g., Fig. 5) would then indicate that the pore size distribution in Vycor has a very sharp cutoff at some maximum. This is quite plausible given the manufacturing process in which a spinodal decomposition is halted at some stage and then one phase is leached. It is also consistent with evidence from mercury intrusion porosimetry.

This interpretation of the freezing results does not provide an obvious explanation for the hysteresis when the solid in the pores is melted. One possible explanation is that the pores are more like cylinders than spheres. The solid may still nucleate as a sphere, in accordance with Eqs. (1) and (2), but it could then expand along the pore, forming a cylindrical frozen region. Since a long cylinder has a smaller surface-to-volume ratio than a sphere of the same radius, it will be more thermodynamically stable and so melt at a higher temperature. This simple model would predict the depression of the melting temperature to be two-thirds as large as the freezing-point depression, in rough agreement with our observations. Another possibility involves the narrow necks between pores. Even if neighboring pores freeze independently, further cooling will cause the frozen region to extend further into the necks between pores until they touch. When separate

solid regions join, some surface area will be eliminated, along with its associated free energy, again stabilizing the solid to higher temperatures. Finally, it has been suggested[18,26] that there may be a highly dislocated or amorphous layer on the pore surfaces which rearranges once the fluid in a pore freezes, lowering the interfacial free energy which was responsible for the depression of freezing. In all of these pictures, if there is a distribution of pore sizes, the largest will be the first to freeze and the last to melt, and so the behavior shown in Figs. 8 and 9 is not surprising.

It is difficult to decide between such qualitative explanations of the hysteresis. Certainly, neutron scattering from oxygen and deuterium in Vycor[19] shows significant amorphous components, larger for deuterium than for oxygen, which may be related to the relatively large undercooling possible with hydrogen. These measurements also show crystalline peaks whose widths indicate crystallite sizes in the frozen state which are on the order of 40–70 nm, considerably larger than the pore sizes in Vycor. This would appear to suggest that, once formed, a solid region can propagate through necks to several neighboring pores. However, even if adjacent pores froze initially with different crystallographic orientations, the rapid vacancy motion evident in the ultrasonic measurements would allow rapid annealing which could reorient crystallites over substantial regions. To really determine the origin of the hysteresis, we plan to make freezing and melting measurements in materials with different and better defined pore geometries.

## ACKNOWLEDGMENTS

This work was supported by grants from the Natural Sciences and Engineering Research Council of Canada and The Petroleum Research Fund, administered by the American Chemical Society and by the National Science Foundation under Grants Nos. DMR-8701651 and DMR-9008461. We would like to thank M. Shafer and D. D. Awschalom for providing us with the xerogel sample and Karl Unruh for helpful conversations.

*Present address: AT&T Bell Laboratories, Murray Hill, New Jersey 07974.

[1]M. H. W. Chan, K. I. Blum, S. Q. Murphy, G. K. S. Wong, and J. D. Reppy, Phys. Rev. Lett. **61**, 1950 (1988); D. Finotello, K. A. Gillis, A. P. Y. Wong, and M. H. W. Chan, *ibid.* **61**, 1954 (1988); N. Mulders and J. R. Beamish, *ibid.* **62**, 438 (1989); G. K. S. Wong, P. A. Crowell, H. A. Cho, and J. D. Reppy, *ibid.* **65**, 2410 (1990); N. Mulders, R. Mehrotra, L. S. Goldner, and G. Ahlers, *ibid.* **67**, 695 (1991); M. Larson, N. Mulders, and G. Ahlers, *ibid.* **68**, 3896 (1992).

[2]A. P. Y. Wong and M. H. W. Chan, Phys. Rev. Lett. **65**, 2567 (1990).

[3]J. V. Maher, W. I. Goldburg, D. W. Pohl, and M. Lanz, Phys. Rev. Lett. **53**, 60 (1984); K.-Q. Xia and J. V. Maher, Phys. Rev. A **36**, 2432 (1987); **37**, 3626 (1988); M. C. Goh, W. I. Goldburg, and C. M. Knobler, Phys. Rev. Lett. **58**, 1008 (1987); P. Wiltzius, S. B. Dierker, and B. S. Dennis, *ibid.* **62**, 804 (1989); S. B. Dierker and P. Wiltzius, *ibid.* **66**, 1185 (1991).

[4]G. Litvan and R. McIntosh, Can. J. Chem. **41**, 3095 (1963).

[5]J. L. Tell and H. J. Maris, Phys. Rev. B **28**, 5122 (1983).

[6]R. H. Torii, H. J. Maris, and G. M. Seidel, Phys. Rev. B **41**, 7167 (1990).

[7]S. R. Haynes, D. F. Brewer, and A. L. Thomas, Jpn. J. Appl. Phys. **26**, 301 (1987); D. F. Brewer, J. Rajendra, N. Sharma, A. L. Thomson, and Jin Xin, Physica B **165&166**, 551 (1990); **165&166**, 577 (1990).

[8]D. F. Brewer, J. Rajendra, N. Sharma, and A. L. Thomson, Physica B **165&166**, 569 (1990).

[9]K. M. Unruh, B. M. Patterson, and S. I. Shah, J. Mater. Res. **7**, 214 (1992); in *Physical Phenomena in Granular Materials,* edited by G. D. Cody, T. H. Geballe, and P. Sheng, MRS Symposia Proceedings No. 195 (Materials Research Society, Pittsburgh, PA, 1990), p. 567.

[10]C. L. Jackson and G. B. McKenna, J. Chem. Phys. **93**, 9002 (1990).

[11]R. Mu and V. M. Malhotra, Phys. Rev. B **44**, 4296 (1991).

[12]J. R. Beamish, A. Hikata, L. Tell, and C. Elbaum, Phys. Rev. Lett. **50**, 425 (1983); J. R. Beamish, N. Mulders, A. Hikata, and C. Elbaum, Phys. Rev. B **44**, 9314 (1991).

[13]E. D. Adams, K. Uhlig, Y.-H. Tang, and G. E. Haas, Phys. Rev. Lett. **52**, 2249 (1984); J. Low Temp. Phys. **66**, 85 (1987).

[14]S. R. Haynes, N. Sharma, D. F. Brewer, and A. L. Thomson, Jpn. J. Appl. Phys. **26**, 299 (1987).

[15]M. Hiroi, T. Mizusake, T. Tsuneto, A. Hirai, and K. Eguchi, Phys. Rev. B **40**, 6581 (1989).

[16]Cao Lie-zhao, D. F. Brewer, C. Girit, E. N. Smith, and J. D. Reppy, Phys. Rev. B **33**, 106 (1986).

[17]M. Shimoda, T. Mizusake, M. Hiroi, A. Hirai, and K. Eguchi, J. Low Temp. Phys. **64**, 285 (1986); Y. Kondo, Y. Kodama, Y. Hirayoshi, T. Mizusake, A. Hirai, and K. Eguchi, Jpn. J. Appl. Phys. **26**, 303 (1987).

[18]D. D. Awschalom, M. R. Arai, and S. Gregory, Phys. Lett. **95A**, 385 (1983); J. Warnock, D. D. Awschalom, and M. W. Shafer, Phys. Rev. Lett. **57**, 1753 (1986); D. D. Awschalom and J. Warnock, Phys. Rev. B **35**, 6779 (1987).

[19]P. E. Sokol, W. J. Ma, K. W. Herwig, W. M. Snow, Y. Wang, J. Koplik, and J. R. Banavar, Appl. Phys. Lett. **61**, 777 (1992).

[20]M. J. Benham, J. C. Cook, J-C. Li, D. K. Ross, P. L. Hall, and B. Sarkissian, Phys. Rev. B **39**, 633 (1989).

[21]Vycor 7930 "Thirsty Glass" from Corning Glass. The pore structure of this glass has been characterized by many techniques, including small-angle neutron scattering. See, e.g., P. Wiltzius, F. S. Bates, S. B. Dierker, and G. D. Wignall, Phys. Rev. A **36**, 2991 (1987).

[22]The xerogel samples were provided by M. Shafer and D. D. Awschalom of IBM, Yorktown Heights. The manufacture and characterization of these materials is described in M. W. Shafer, D. D. Awschalom, J. Warnock, and G. Ruben, J. Appl. Phys. **61**, 5438 (1987).

[23]P. F. Sullivan and G. Seidel, Phys. Rev. **173**, 679 (1968).

[24]F. R. N. Nabarro (unpublished); C. Herring, J. Appl. Phys. **21**, 437 (1950); see also J.-P. Poirier, *Creep of Crystals* (Cambridge University Press, London, 1985).

[25]A. V. Chadwick and H. R. Glyde, in *Rare Gas Solids,* edited by M. L. Klein and J. A. Venables (Academic, New York, 1977), Vol. II.

[26]J. G. Dash, Phys. Rev. B **25**, 508 (1982).